

Beyond [cls]: Exploring the true potential of Masked Image Modeling representations

Marcin Przewięźlikowski^{1,2*} Randall Balestriero³ Wojciech Jasiński^{2,4} Marek Śmieja¹ Bartosz Zieliński^{1,2}
¹Jagiellonian University ²IDEAS NCBR ³Brown University ⁴AGH University of Science and Technology

Abstract

Masked Image Modeling (MIM) has emerged as a popular method for Self-Supervised Learning (SSL) of visual representations. However, for high-level perception tasks, MIM-pretrained models offer lower out-of-the-box representation quality than the Joint-Embedding Architectures (JEA) – another prominent SSL paradigm. To understand this performance gap, we analyze the information flow in Vision Transformers (ViT) learned by both approaches. We reveal that whereas JEAs construct their representation on a selected set of relevant image fragments, MIM models aggregate nearly whole image content. Moreover, we demonstrate that MIM-trained ViTs retain valuable information within their patch tokens, which is not effectively captured by the global [cls] token representations. Therefore, selective aggregation of relevant patch tokens, without any fine-tuning, results in consistently higher-quality of MIM representations. To our knowledge, we are the first to highlight the lack of effective representation aggregation as an emergent issue of MIM and propose directions to address it, contributing to future advances in Self-Supervised Learning¹.

1. Introduction

Self-supervised learning (SSL) [9] has emerged as a powerful learning paradigm, enabling models to learn useful representations from unlabeled data. In computer vision, there are currently two dominant SSL paradigms: Joint-embedding architectures (JEA): [13, 14, 16–19, 29, 32, 42, 62, 65], and Masked Image Modeling (MIM) [4, 5, 10, 33, 47, 58]. Image encoders pretrained with JEAs optimize the objective of producing similar embeddings from multiple views of the same image, which are typically constructed using data augmentations [16]. An example of a JEA is Momentum Contrastive Learning (MoCo) [32], which enforces the similarity of embeddings through a contrastive objective [41]. On the other hand, MIM approaches task image encoders with reconstructing missing pixels (or high-level representations) of images with occluded fragments [55]. The most

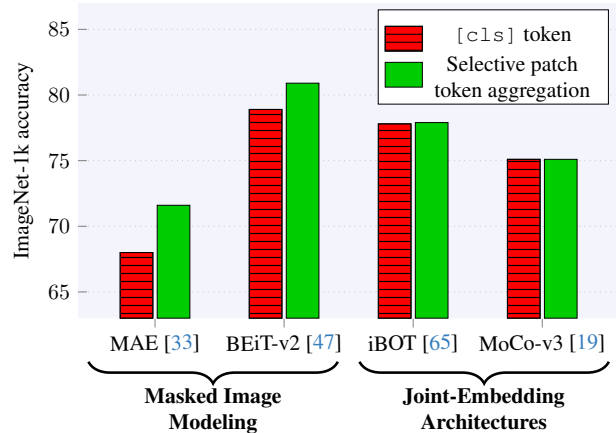


Figure 1. The global [cls] tokens in Vision Transformers trained with Masked Image Modeling (MIM) overlook specific information embedded within the patches, which can enhance performance on high-level perception tasks. Our analysis reveals that this challenge of representation aggregation is inherent to MIM and does not manifest in Joint-Embedding Architectures (JEA).

popular MIM implementation is the Masked Autoencoder (MAE) [33].

Although JEA models frequently offer superior out-of-the-box representation quality, they have several well-known limitations. Firstly, their invariance objectives typically rely on data augmentations that need to be carefully designed depending on the expected target tasks [11, 51, 57]. Moreover, JEA training often implicitly assumes the curation and similar distribution of the pretraining and target data sets [3, 42]. In contrast, MIM approaches rely on a more generic pretext task, but perform worse empirically, with the underlying causes still not fully understood [8, 45, 63].

In this paper, we aim to understand the fundamental differences between the representations learned by JEA and MIM by examining the flow of information between tokens inside Vision Transformers (ViT) [24] pretrained with both paradigms. We are especially interested in how different SSL techniques shape the representations of the so-called [cls] tokens – commonly treated in ViTs as the global image descriptors [14, 24, 33].

*marcin.przewiezlikowski@doctoral.uj.edu.pl

¹Code shall be released at github.com/gmum/beyond_cls.

We find that contrary to JEAs, the `[cls]` token of MAE is ineffective at aggregating the relevant information, which may be a cause for the performance gap between models trained with both approaches (see Fig. 2). However, although the `[cls]` token in MIM models has limitations, the patch tokens of such models contain more high-level information than previously thought. We demonstrate this by aggregating them into representations of superior quality than the `[cls]` token, using straightforward techniques inspired by Multiple-Instance Learning [21, 39]. Such token aggregation consistently improves the high-level representation quality of a wide range of MIM models [4, 33, 47, 56, 58] without fine-tuning of their parameters (see Fig. 1), revealing a general issue with the MIM pretraining paradigm. We conclude with recommendations for advancing MAE and MIM-based approaches, offering insights into improving their high-level representation capabilities.

Our contributions can be summarized as follows:

- We analyze the information flow inside the widely used models trained with SSL and reveal that the attention mechanism of JEAs is selective, whereas the MAE aggregates information from the majority of image patches.
- We reveal that patch tokens of MIM-trained models contain more high-level information than was previously thought. We demonstrate this by aggregating the relevant patch tokens into representations of consistently better quality than those formed by the `[cls]` tokens.
- Our empirical evaluation of MIM and JEA-pretrained models indicates that the lack of representation aggregation is an inherent issue in MIM. With this observation, we shed new light on this SSL pre-training paradigm and provide key insights for its future advancements.

2. Related works

Self-supervised learning (SSL) of visual representations has lately been of great interest to the scientific community, opening up the possibility of learning powerful models without labeled data [1, 9]. SSL requires an appropriate *pretext task* which replaces a data-defined objective, and over the years, a plethora of such tasks have been proposed [23, 27, 40, 64]. In particular, the objective of invariance of representation to data augmentations optimized by Joint-Embedding Architectures (JEA) [13, 14, 16–19, 29, 32, 42, 62, 65], is currently believed to be best-aligned with downstream tasks that require high-level perception, such as image classification. Moreover, in JEA-trained Vision Transformers [24] there emerges an ability to showcase the parts of the images relevant for perception with attention maps [52]. However, JEA approaches require a careful choice of hand-crafted data augmentations [51], and their learned invariance to data perturbations can adversely affect the quality of representations [15, 37, 48, 57]. Moreover,

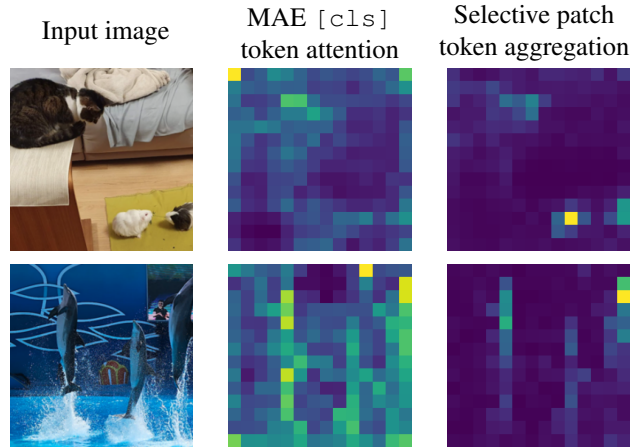


Figure 2. The `[cls]` token of models trained via Masked Image Modeling spreads its attention between a large number of patch tokens (center column), including these containing information irrelevant for high-level perception. We show that selective aggregation of the relevant patch tokens (right column) is essential for forming high-level image representations of good quality.

JEA pretraining implicitly assumes a similar distribution of its pretraining and downstream task data [3], causing a need for additional dataset curation [42]. Therefore, development of SSL paradigms alternative to JEAs is an active line of research [4, 26, 53]. In this work, we study one such paradigm, Masked Image Modeling (MIM) [55], which we compare to JEA, especially in terms of the attention mechanism [52] behaviour developed by the two techniques.

Masked image modeling (MIM) [54, 55] is a technique of self-supervised pretraining of image representations by learning to reconstruct corrupted images or their high-level representations. Recent years have seen a renewed interest in MIM approaches, due to their natural applicability to Vision Transformers [5, 24, 33, 58], as well as the successes of Masked Modeling in pretraining of Large Language Models [22]. In particular, Masked Autoencoders (MAE) [33] have proved to be a powerful foundation for diverse visual tasks, including but not limited to segmentation [49], active visual exploration [43, 44], and medical imaging [66]. Yet, as of now, models trained via MIM have not matched the out-of-the-box quality of the Joint-Embedding Architectures (JEA) in high-level visual perception tasks [8, 33]. Our work investigates this problem and describes the crucial role of the attention mechanism emergent in JEA, but not in the MIM approaches.

Comparisons of Masked Image Modeling and Joint-Embedding Architectures have been the focus of several works, which tried to understand the differences and combine the advantages of both paradigms [8, 36, 45, 63].

The authors of [36, 63] frame MIM as a JEA that learns invariance to image occlusions, but find its representation to be less expressive than in other JEAs. A theoretical study of learning by reconstruction, conducted in [8], shows that data features required for reproducing pixels are misaligned with those needed for high-level perception. As a solution, multiple works propose shifting the prediction target from low-level pixels to higher-level image features, such as Histograms of Oriented Gradients [56] or latent representations [4, 47, 60], akin to the JEA objective. Finally, [45] thoroughly compare the properties of MIM and JEA-trained models including, similarly to us, the attention mechanisms of their patch tokens. They find that whereas JEAs form global and homogeneous attention maps, the attention of MIM patch tokens is more localized. Furthermore, [34, 59] show that MIM-pretrained transformers produce attention patterns that capture diverse image aspects, useful for tasks which require spatial understanding of images. Our work significantly extends these studies – we analyze the [cls] and patch representations of models trained with both paradigms and provide a detailed description of the information flow within them. We find that the attention mechanism emergent in MIM models imposes limitations that prevent these models from realizing their full potential in high-level perception tasks. Although this consequence of masked pretraining has previously been hinted at in the language models literature [25], to the best of our knowledge, it has not yet been discussed in the context of computer vision. While [25] address this with a modified pretraining scheme, we present a proof-of-concept that patch tokens of unmodified MIM models carry more information and can be combined into global image representations of superior quality than previously thought.

3. Preliminaries

In this section, we recall the basic Vision Transformer (ViT) architecture [24], and the Masked Autoencoder (MAE) [33] – the most popular Masked Image Modeling technique.

3.1. Vision Transformers

Image processing by ViT begins by dividing and flattening an image $\mathbf{x} \in \mathbb{R}^{H \times W \times C}$ into a sequence of N non-overlapping *patches* $\mathbf{x}_p \in \mathbb{R}^{N \times (P^2 \cdot C)}$, where (P, P) is the resolution of a patch and $N = \frac{HW}{P^2}$. Next, a linear projection layer $e : \mathbb{R}^{(P^2 \cdot C)} \rightarrow \mathbb{R}^D$ transforms each patch into a D -dimensional embedding to which appropriate positional encoding vectors $\mathbf{p} \in \mathbb{R}^{N \times D}$ [24] are added. We refer to the result of these operations as *patch tokens*:

$$\mathbf{z}_p = e(\mathbf{x}_p) + \mathbf{p} \in \mathbb{R}^{N \times D}. \quad (1)$$

We also define a learnable [cls] token $\mathbf{x}_{cls} \in \mathbb{R}^D$, which is prepended to \mathbf{z}_p ². The first ViT block input is defined as:

$$\mathbf{z}_0 = [\mathbf{x}_{cls}; \mathbf{z}_p] \in \mathbb{R}^{(N+1) \times D} \quad (2)$$

The l -th ViT block transforms tokens \mathbf{z}_{l-1} into tokens \mathbf{z}_l . Each of the L blocks is a sequence of Multihead Self-Attention (MSA) [52] and MLP layers. For both MSA and MLP, the input is first normalized with LayerNorm [6], and the output of the layer is summed with the unnormalized input, forming a residual connection [30].

Multihead Self-attention (MSA) [52] is a key component of ViT, which allows for exchanging the image information between tokens. It consists of h self-attention heads, each of which separately transforms the sequence of $(N + 1)$ input tokens into a sequence of output tokens of the same length. A self-attention head creates three linear projections of the input, $\{\mathbf{q}, \mathbf{k}, \mathbf{v}\} \in \mathbb{R}^{(N+1) \times (D/h)}$ and computes the self-attention map $\mathbf{a} \in [0, 1]^{(N+1) \times (N+1)}$:

$$\mathbf{a} = \text{softmax}\left(\frac{\mathbf{q}\mathbf{k}^T}{\sqrt{D/h}}\right), \quad (3)$$

Output tokens $\mathbf{o} \in \mathbb{R}^{(N+1) \times (D/h)}$ are calculated as $\mathbf{o} = \mathbf{a}\mathbf{v}$, i.e. the sums of \mathbf{v} weighted by subsequent rows of \mathbf{a} . Next, the output tokens of each self-attention head are concatenated along their token dimension and projected through a linear layer to form the final output of the MSA.

Final Vision Transformer representation \mathbf{z}_L consists of $(N + 1)$ tokens of shape D . In high-level perception tasks such as image classification, the most common strategy is to use only the [cls] token output of the final ViT block ($\mathbf{z}_{L,0}$) as the representation of the entire image which serves as an input to the classifier [14, 24, 63]. The same approach is used in JEA pretraining, where the invariance objective is imposed on the [cls] representations (typically followed by a projector network [12, 16]), while patch tokens are discarded [14, 19]. An alternative strategy is to summarize the image representation as the average value of patch tokens, i.e. $\sum_{i=1}^N \frac{\mathbf{z}_{L,i}}{N}$, sometimes even removing the [cls] token from the model [2, 33]. However, this typically leads to representations of worse quality [24].

3.2. Masked Image Modeling

Masked Image Modeling (MIM) [54, 55] is a paradigm of learning representations through the task of image inpainting (masking random contents of images and training a model to reconstruct them). This approach is straightforward to apply in Vision Transformers because masking can

²For convenience of notation, the [cls] token will have the index of 0, and patch tokens will have the indices $\in 1 \dots N$.

be implemented by randomly removing a subset of patch tokens. Among the various MIM implementations [5, 58], the Masked Autoencoder (MAE) [33] has emerged as one of the most popular frameworks.

Masked Autoencoder (MAE) consists of two ViTs – an encoder f and decoder g . During MAE pretraining, we divide the image into patch tokens \mathbf{z}_p , remove random subset of tokens, and then process the remaining ones through the encoder. The tokens to be removed are selected by a random binary mask $m \in \{0, 1\}^N$, where 0 is drawn with the probability of ρ (mask ratio) and denotes the dropped tokens. In consequence, the input and output sequences of f consist of $(1 + N \cdot (1 - \rho))$ tokens (the [cls] token and $N \cdot (1 - \rho)$ patch tokens).

Before processing the output of f through the decoder³ g , we complement it with $N \cdot \rho$ identical *mask tokens* $\mathbf{z}_{mask} \in D$, such that the placement of mask tokens reflects the placement of tokens removed by mask m . The decoder adds an appropriate positional embedding to both, encoded and mask tokens. After obtaining the output sequence of g , we discard the [cls] token and project the N patch tokens into the sequence $\hat{\mathbf{x}}_p \in \mathbb{R}^{N \times (P^2 \cdot C)}$, i.e. of the same size as the image patches \mathbf{x}_p .

The objective function of MAE is defined as the mean squared error between the image pixels and predicted pixels, calculated at the patches that were randomly dropped by mask m :

$$\mathcal{L}_{MAE} = \mathbb{E}_{\mathbf{x}} \|\mathbf{x}_p[1 - m] - \hat{\mathbf{x}}_p[1 - m]\|^2. \quad (4)$$

Numerous works propose to replace the MAE prediction target with higher-level representations of patches. Such targets can be formed from low-variance image components [8, 56], or latent representations of an image encoder [4, 10, 47, 60]. However, the reconstruction objective is typically applied to the patch tokens, whereas the [cls] representation does not optimize any objective. This raises the question of what representation is formed by [cls], and its role in the information flow between the tokens.

4. Information flow in Self-supervised ViTs

Despite not optimizing any explicit objective, the [cls] token in Masked Image Models has been shown to capture a representation that can, to some extent, serve as a global image descriptor [33, 58]. This motivates the question: **How are the representations exchanged between the patch and [cls] tokens in Masked Image Modeling, and how does it relate to methods where the [cls] representation optimizes a specific objective?**

³For simplicity of notation, we assume that the encoder and decoder have equal embedding sizes and numbers of layers, denoted by D and L , respectively. In practice, if the embedding sizes are not equal, we prepend the decoder with an appropriate linear projection.

To answer this, we explore the self-attention mechanism in Vision Transformers, as it is the only mechanism through which the [cls] token can acquire information from image patches.

Experimental setup. In self-attention, each token either recycles its representation by attending to itself or gathers the representations of other tokens by attending to them. We are interested in finding out the degree of recycling, as well as whether tokens attend to other tokens in any structured way. We thus measure the following properties of self-attention maps during inference:

- **for the [cls] token:**

- the attention of [cls] to itself (Fig. 3)
- the entropy of attention of [cls] to the patch tokens (Fig. 4)

- **for each patch token:**

- the attention of the token to itself, relative to its total attention to all patch tokens (Fig. 5)
- entropy of attention of the token to all patch tokens (Fig. 6)

The entropy of an i -th token’s attention to patch tokens (i.e. the $\mathbf{a}_{i,1:N}$ vector) is given by the Shannon entropy of its normalized values:

$$\mathbb{H}(\mathbf{a}'_i) = - \sum_{j=1}^N \mathbf{a}'_{i,j} \cdot \log(\mathbf{a}'_{i,j}), \quad (5)$$

where $\mathbf{a}'_{i,1:N} = \frac{\mathbf{a}_{i,1:N}}{\sum_{j=1}^N \mathbf{a}_{i,j}}$. We measure this above values for

each self-attention head in each ViT block and report the average results for each block. The inference is performed on the ImageNet-1k validation dataset (with 50,000 images).

To comprehensively compare the Masked Image Modeling and Joint-Embedding paradigms, we analyze the ViT-Base models pretrained with MAE [33], DINO [14], MoCo-v3 [19], and iBOT [65]. We conduct a similar analysis of ViT-Small and ViT-Large models in the Appendix. For all models, we use the pre-trained parameters publicly provided by their respective authors. Moreover, we analyze the MAE fine-tuned for ImageNet-1k classification on top of the [cls] token features, to understand how the MAE attention mechanism changes after fine-tuning to the high-level perception task. Finally, we analyze the model trained for ImageNet-1k classification from scratch to assess the role of MAE initialization in supervised tasks.

4.1. Analysis of the [cls] token

We observe significant differences in the behavior of [cls] tokens between models pretrained with MAE and those pretrained with joint-embedding methods, particularly in how they attend to themselves and the patch tokens. Our key findings are presented in the following paragraphs.

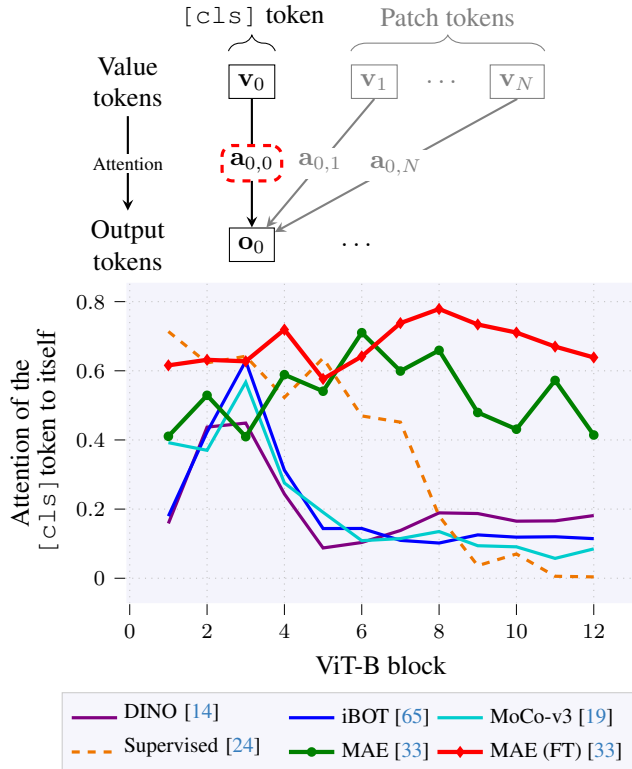


Figure 3. Attention of the $[\text{cls}]$ token to itself is much higher in MAE, than in the JEA ViTs. As opposed to JEA, where the $[\text{cls}]$ tokens gather a large amount of information from the patch tokens, the MAE $[\text{cls}]$ tokens primarily recycles its own representation.

The $[\text{cls}]$ token of MAE attends primarily to itself.

The first noticeable difference, depicted in Fig. 3, is in the amount of attention assigned by $[\text{cls}]$ token to itself instead of the patch tokens. Whereas in ViTs trained via JEA and supervised approaches, this value decreases with the depth of the encoder, in MAE the $[\text{cls}]$ consistently assigns roughly half of its attention to its own representation from the previous ViT blocks. This suggests that the $[\text{cls}]$ token of MAE primarily recycles the already gathered information, reducing the impact of high-level patch representations. On the other hand, $[\text{cls}]$ tokens in ViTs trained with supervised and joint-embedding approaches are more likely to update their representations with information extracted from patch tokens. Counterintuitively, fine-tuning the $[\text{cls}]$ representation of MAE for classification *increases* the amount of attention it assigns to itself. We hypothesize this is due to the convergence dynamic of MAE pretraining, where the network reaches a state significantly different from one obtained by supervised training from scratch. During fine-tuning, the model optimizes locally around this MAE-induced state, where maintaining self-focused attention retains information beneficial for downstream tasks.

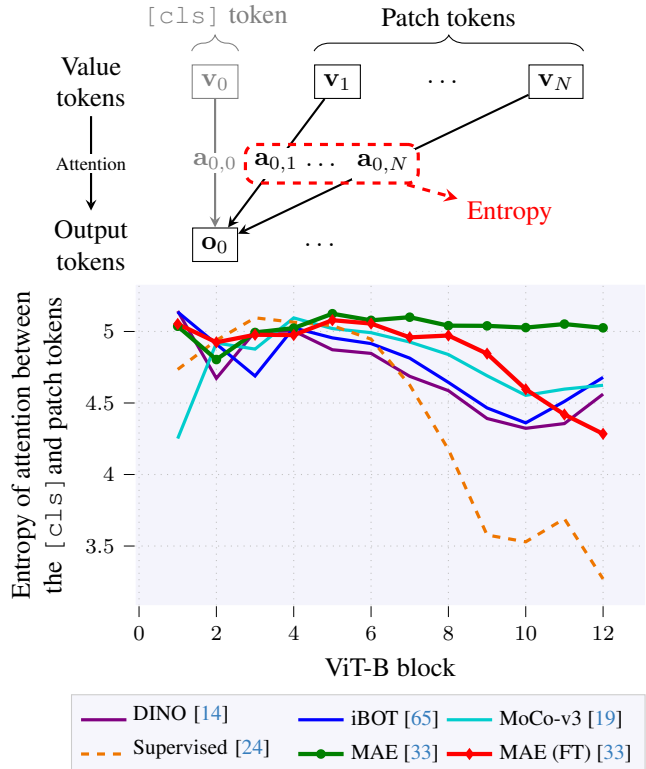


Figure 4. Entropy of attention between the $[\text{cls}]$ and patch tokens. In MAE, its value reaches almost the maximal possible level. In other models, it decreases in the deeper model blocks, indicating that the $[\text{cls}]$ token attends to different patches in a more selective manner. Fine-tuning of MAE decreases this entropy, indicating that selective attention to patch tokens is crucial for good perception.

The $[\text{cls}]$ token of MAE attends to the patches too uniformly to select only the relevant ones.

In Fig. 4, we measure the entropy of attention between the $[\text{cls}]$ and patch tokens, as denoted in Eq. (5). In MAE, the mean entropy of attention maps remains stable with the value close to 5 throughout the subsequent ViT blocks. On the other hand, in the remaining ViTs the mean entropy decreases with ViT depth to values around 4.5 for joint-embedding models and the fine-tuned MAE, and even lower, 3.5 for the supervised ViT. The upper bound of the entropy of a discrete distribution with 196 elements (i.e. the number of patch tokens) equals approximately 5.27. Therefore, $\mathbb{H} = 5$ and $\mathbb{H} = 4.5$ roughly correspond to uniformly attending to 150 and 85 (out of 196) tokens, respectively.

We can thus see that the attention of MAE is spread over a much larger amount of tokens than in joint-embedding and supervised ViTs. Moreover, fine-tuning of MAE decreases the entropy to a similar level as joint-embedding ViTs. Given that the $[\text{cls}]$ representations in joint-embedding ViTs

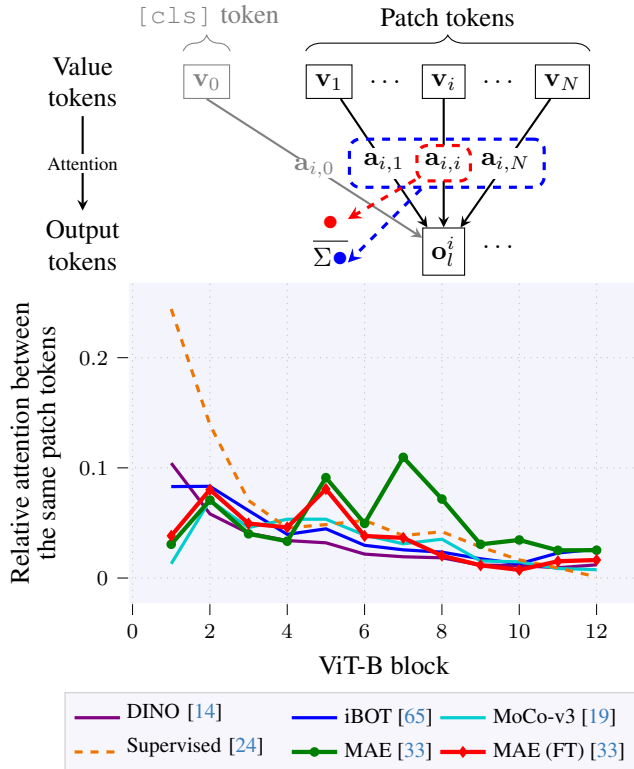


Figure 5. Attention of the patch tokens to themselves, relative to the total attention assigned to all patch tokens. In the latter MAE blocks, patch tokens seem to assign the largest amount of relative attention to themselves, compared to the tokens of JEA.

and fine-tuned MAEs are much better suited for perception compared to their MAE counterparts, we hypothesize that their ability to selectively focus on relevant patch tokens is a crucial property that does not naturally emerge in the MAE framework.

4.2. Analysis of the patch tokens

Next, we focus on the patch tokens of Vision Transformers. To this end, we measure the value of self-attention the patch assigns to itself (relative to the total attention assigned to all patch tokens) and the entropy of its attention to all patches.

The patch tokens of MAE assign more attention to themselves. Fig. 5 shows that the patches of MAE assign a larger amount of attention to themselves, compared to their joint-embedding, fine-tuned, and supervised counterparts. This behavior suggests that patch tokens in MAE are less likely to exchange information with other patches.

Patch tokens of MAE attend to patches more selectively than those of JEA. The above findings are further rein-

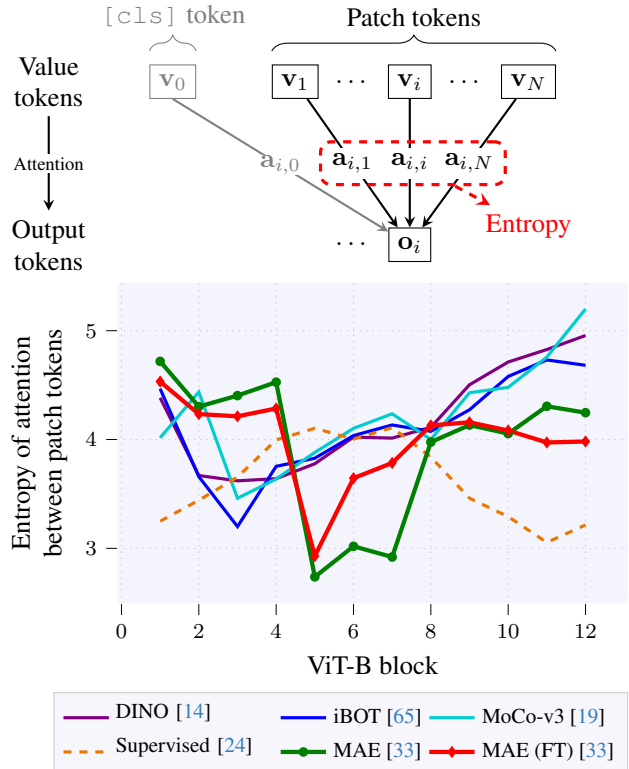


Figure 6. Entropy of patch tokens attention to patch tokens. In MAE, the patch tokens attend to other patches with lower entropy than in JEA, indicating that they form a representation of local image fragments.

forced by Fig. 6, which depicts the entropy of attention between patch tokens. Contrary to the `[cls]` token, patch tokens of MAE attend to other patches with lower entropy than the patches of joint-embedding models. This suggests that patches in MAE mix their representations more selectively than those of the models trained with JEA. Our findings align with [35], who found that MAE patches form clusters matching the semantics of the image contents, as well as [45], who showed that the attention of patch tokens in MAE is sparse and localized, whereas the patch attention maps of JEA tend to cover the entire objects and are thus more homogeneous. This indicates that the patch tokens of MAE possess more diverse representations that describe their local image fragments.

4.3. Discussion

Our analysis of the attention mechanism in Self-supervised Vision Transformers reveals several properties apparent for JEA-trained models, but not for the MAE. The `[cls]` token of JEA attends strongly to the patch tokens, meaning that it is prone to update its representation throughout all ViT blocks. On the other hand, the `[cls]` token of the MAE

largely recycles its representations from shallower blocks. Moreover, the attention mechanism emergent in JEA is more selective of patches relevant for global image representation compared to the MAE, as evidenced by the difference in the entropy of attention between their [cls] and patch tokens. As for the patch tokens, we observe that in MAE they attend more strongly to themselves instead of other patches, whereas in JEA, their attention is spread among more patches, as evidenced by higher entropy.

Crucially, fine-tuning of the MAE [cls] representation for classification increases the selectiveness of the [cls]-patch attention, and the relative self-attention of patch tokens to the levels observed in JEA. This leads us to hypothesize that these properties of Vision Transformers are crucial for forming a good quality global image representation. Although MAE patches contain the representation of their local contents [35, 45], the [cls] token treats them too uniformly, absorbing both relevant and redundant information.

5. Masked Image Models Benefit from selective token aggregation

Knowing already that the [cls] token of masked models tends to recycle its own low-level representations, attends to a large number of diverse patches, and forms a global representation of poor quality, we ask: **Do the patch tokens of MIM models contain high-level information that is lost when aggregating them by the [cls] token?**

To answer this, we seek to establish an alternative aggregation function $s : \mathbb{R}^{N \times D} \rightarrow [0, 1]^N$ that, given the sequence of patch tokens from the L -th ViT encoder block ($\mathbf{z}_{L,1:N}$), predicts a vector $\mathbf{s} \in [0, 1]^N$ of scores used for weighted summation of patch tokens, corresponding to the attention mechanism [7]. The weights of \mathbf{s} identify the key patch tokens, aggregating them into the representation $\mathbf{z}_{\text{select}} = \sum_{i=1}^N s_i \mathbf{z}_{L,i} \in \mathbb{R}^D$, which can then be used as a drop-in replacement for the [cls] representation.

The existence of a function s that aggregates the patches into a representation better than the [cls] token would indicate that the MIM patch tokens indeed contain high-level information that was not absorbed by [cls], supporting the above hypothesis.

For this purpose, we employ Attention-based Multiple Instance Learning Pooling (AbMILP) [39] to learn an aggregation of patch tokens during linear evaluation. To formally recall AbMILP, given a set of vectors (in our case, the patch tokens), it predicts the aggregation weights by applying a model $t : \mathbb{R}^D \rightarrow \mathbb{R}$ to each vector, followed by softmax:

$$\mathbf{s}_i^{\text{AbMILP}} = \frac{\exp(t(\mathbf{z}_{L,i}))}{\sum_{j=1}^N \exp(t(\mathbf{z}_{L,j}))}. \quad (6)$$

The remainder of this section is dedicated to the experimental evaluation of Self-supervised Vision transformers equipped with the above token aggregation mechanism. We explore the design of the t function in AbMILP and alternative token aggregation functions in the Appendix.

Experimental setup. We are interested in measuring the out-of-the-box high-level perception capabilities of Vision Transformer representations. We evaluate this in terms of their performance on the ImageNet-1k classification task [50]. Our evaluation follows several principles:

- We evaluate models initialized with ImageNet-1k-pretrained parameters made publicly available by the authors of various Self-supervised algorithms [4, 14, 19, 24, 33, 47, 58, 65, 66]⁴.
- We do not fine-tune the parameters of evaluated models, but only train the classification heads that use their final representations.
- We do not use techniques for improving the linear probing performance, such as combining the representations from other-than-last ViT blocks [14, 47]⁵.

In practice, our evaluation follows the MAE linear probing protocol [33]: We augment the images only by random cropping, use the batch size of 16,384, and train the classifier head for 90 epochs (50 in the case of ViT-Large and Huge) with the LARS optimizer [28], the base learning rate of 0.1 with cosine decay and 10 epochs of warmup, optimizer momentum of 0.9, and no weight decay.

The classifier is a single linear layer that maps the representation vectors of the shape D to logits of the shape K , equal to the number of classes (in our case, $K = 1,000$). The AbMILP-based token aggregator consists of a single linear layer that maps the representation vectors of shape D into scalars (i.e. the model t in Eq. (6)). The number of trainable parameters is thus increased by a negligible margin, from $(D \cdot (K + 1))$ to $(D \cdot (K + 1) + D + 1)$.

5.1. Evaluation of the AbMILP token aggregation

We evaluate the quality of representations formed by the [cls] token, average patch representation, and aggregating patch tokens with AbMILP [39] in terms of classification performance on the ImageNet-1k dataset [50], and report the results averaged over 3 random seeds in Table 1.

The MAE patch representation accumulated by AbMILP yields results superior to those of the [cls] and average patch representations. We observe this consistently in all tested ViT architectures, from Small to Huge [24]. The most drastic increase in quality can be observed in SimMIM [58]. We speculate that, due to processing mask tokens by the SimMIM encoder, the MIM objective promotes information

⁴Due to the lack of publicly available parameters of ViT-S trained with MAE, we train this model with the same procedure as used for ViT-B [33].

⁵When using the SimMIM parameters, we use the representations from the 8-th ViT block, as recommended by the authors [58].

	Encoder		Aggregation method		
	Initialization	ViT type	Avg. patch	[cls]	AbMILP
Masked Img. Modeling	MAE [33]	ViT-S	47.1	47.4	54.4
	MAE [33]	ViT-B	65.8	67.8	71.6
	MAE [33]	ViT-L	73.0	75.8	77.4
	MAE [33]	ViT-H	73.8	77.0	78.1
	SimMIM [58]	ViT-B	54.3	51.5	62.8
	MaskFeat [56]	ViT-B	56.9	62.9	66.6
	BEIT-v2 [47]	ViT-B	78.5	78.9	80.9
	I-JEPA [4]	ViT-H	77.7	–	79.2
JEA	DINO [14]	ViT-B	71.1	76.6	74.7
	MoCo-v3 [19]	ViT-B	71.1	75.1	75.1
	iBOT [65]	ViT-B	75.0	77.8	77.9
	MAE (FT) [33]	ViT-B	76.6	80.0	79.1
	Supervised [24]	ViT-B	80.5	80.6	80.6

Table 1. Linear probing accuracy on ImageNet-1k [50] of Vision Transformers with different techniques of forming global image representation. In Masked Image Models, patch tokens aggregated via AbMILP [39] consistently produce global representations that are more useful for high-level perception than those obtained from the [cls] and naively averaged patch tokens. On the other hand, we do not observe such a performance gap in models pretrained via Joint-embedding or Supervised approaches.

flow primarily from patch to mask tokens, but not between different patches, resulting in poor global representation aggregation. The AbMILP token selection also improves the representations of BEIT-v2 [47] and I-JEPA [4]. This shows that MIM models that were pre-trained with high-level latent representation prediction targets also require appropriate representation aggregation.

Contrary to models trained with MIM, applying the AbMILP token aggregation to models trained with JEA [14, 19, 65] as well as supervised [24], achieves performance on par or worse than the one aggregated by the [cls] token. The only performance improvement can be observed in iBOT [65], which uses mask modeling of its own patch representations as a secondary training objective to JEA. This suggests that in joint-embedding models, the [cls] token is already capable of building global image representations well-suited for high-level perception tasks. We also note that the aggregated patch tokens of JEAs offer higher representation quality than those of the MAE and other MIMs with low-level prediction target [8]. Therefore, the patch representations of MIM models can be less suitable for dense prediction tasks, such as object detection, which we explore in the Appendix.

However, the question of the absolute quality of patch representations is orthogonal to the issue of how they are aggregated, which is the main topic of this work. Among the considered models, only the MIM-pretrained benefit from the selective aggregation, which suggests that the lack of such aggregation is an inherent issue in Masked Image Modeling.

6. Conclusion and future work

This paper presents an in-depth analysis of the information flow in Self-supervised Vision Transformers pretrained with Joint-Embedding Architectures (JEA) and Masked Image Modeling (MIM). We ask why MIM models lag behind JEAs in terms of their quality in high-level perception tasks. We reveal that contrary to JEAs, the [cls] token in MIMs does not selectively aggregate information from patch tokens but spreads its attention to a large number of patches, leading to the accumulation of irrelevant information. Inspired by Multiple-Instance Learning, we next demonstrate that proper aggregation of the information contained in patch tokens consistently improves the quality of representations of multiple MIM models, regardless of whether their original prediction target was low-level pixels or high-level latent representations.

These findings support our hypothesis that a proper, selective aggregation of information stored in the patch tokens is crucial for forming high quality representations in Vision Transformers. Incorporating such a property into the training of future MIM models is an interesting area for future research, that could further improve their perception capabilities. We hope our work will provide a better understanding of Masked Image Modeling and inspire new directions in the development of more powerful visual Self-supervised learning techniques.

Limitations. Our analysis is based on models pretrained by the original authors, which limits our ability to explore model variations or hyperparameter choices, as only a single configuration was provided. Additionally, we have not tested all possible variants of JEA and MIM models, so our findings may not generalize to all configurations.

Impact statement. This work enhances our understanding of Self-Supervised Vision Transformers and opens new avenues for improving MIM models. By highlighting the importance of selective aggregation, it paves the way for future research focused on developing more efficient and effective self-supervised learning techniques, with the potential to significantly advance high-level perception tasks.

Acknowledgements

We thank Marcin Sendera, Adam Pardy, Turhan Can Kargin, Michał Pietruszka, and Klaudia Bałazy for fruitful discussions and feedback during the course of the work.

References

- [1] Saleh Albelwi. Survey on self-supervised learning: Auxiliary pretext tasks and contrastive learning methods in imaging. *Entropy*, 24(4), 2022. 2

- [2] Mahmoud Assran, Mathilde Caron, Ishan Misra, Piotr Bojanowski, Florian Bordes, Pascal Vincent, Armand Joulin, Mike Rabbat, and Nicolas Ballas. Masked siamese networks for label-efficient learning. In *European Conference on Computer Vision*, pages 456–473. Springer, 2022. 3
- [3] Mido Assran, Randall Balestriero, Quentin Duval, Florian Bordes, Ishan Misra, Piotr Bojanowski, Pascal Vincent, Michael Rabbat, and Nicolas Ballas. The hidden uniform cluster prior in self-supervised learning. In *The Eleventh International Conference on Learning Representations*, 2023. 1, 2
- [4] Mahmoud Assran, Quentin Duval, Ishan Misra, Piotr Bojanowski, Pascal Vincent, Michael Rabbat, Yann LeCun, and Nicolas Ballas. Self-supervised learning from images with a joint-embedding predictive architecture. In *Proceedings of the IEEE/CVF Conference on Computer Vision and Pattern Recognition (CVPR)*, pages 15619–15629, 2023. 1, 2, 3, 4, 7, 8
- [5] Sara Atito, Muhammad Awais, and Josef Kittler. Sit: Self-supervised vision transformer. *arXiv preprint arXiv:2104.03602*, 2021. 1, 2, 4
- [6] Jimmy Lei Ba, Jamie Ryan Kiros, and Geoffrey E. Hinton. Layer normalization, 2016. 3
- [7] Bahdanau and others. Neural machine translation by jointly learning to align and translate. In *ICLR*, 2015. 7
- [8] Randall Balestriero and Yann LeCun. How learning by reconstruction produces uninformative features for perception. In *Forty-first International Conference on Machine Learning*, 2024. 1, 2, 3, 4, 8, 14
- [9] Randall Balestriero, Mark Ibrahim, Vlad Sobal, Ari S. Morcos, Shashank Shekhar, Tom Goldstein, Florian Bordes, Adrien Bardes, Grégoire Mialon, Yuandong Tian, Avi Schwarzschild, Andrew Gordon Wilson, Jonas Geiping, Quentin Garrido, Pierre Fernandez, Amir Bar, Hamed Pirsiavash, Yann LeCun, and Micah Goldblum. A cookbook of self-supervised learning. *ArXiv*, abs/2304.12210, 2023. 1, 2
- [10] Hangbo Bao, Li Dong, Songhao Piao, and Furu Wei. Beit: Bert pre-training of image transformers, 2022. 1, 4
- [11] Adrien Bardes, Jean Ponce, and Yann LeCun. Vicregl: Self-supervised learning of local visual features. In *NeurIPS*, 2022. 1
- [12] Florian Bordes, Randall Balestriero, Quentin Garrido, Adrien Bardes, and Pascal Vincent. Guillotine regularization: Why removing layers is needed to improve generalization in self-supervised learning. *Transactions on Machine Learning Research*, 2023. 3
- [13] Mathilde Caron, Ishan Misra, Julien Mairal, Priya Goyal, Piotr Bojanowski, and Armand Joulin. Unsupervised learning of visual features by contrasting cluster assignments. In *Advances in Neural Information Processing Systems*, pages 9912–9924. Curran Associates, Inc., 2020. 1, 2
- [14] Mathilde Caron, Hugo Touvron, Ishan Misra, Hervé Jégou, Julien Mairal, Piotr Bojanowski, and Armand Joulin. Emerging properties in self-supervised vision transformers. In *Proceedings of the International Conference on Computer Vision (ICCV)*, 2021. 1, 2, 3, 4, 5, 6, 7, 8, 12, 14, 17, 18, 19, 20
- [15] Ruchika Chavhan, Jan Stuehmer, Calum Heggan, Mehrdad Yaghoobi, and Timothy Hospedales. Amortised invariance learning for contrastive self-supervision. In *The Eleventh International Conference on Learning Representations*, 2023. 2
- [16] Ting Chen, Simon Kornblith, Mohammad Norouzi, and Geoffrey Hinton. A simple framework for contrastive learning of visual representations. In *Proceedings of the 37th International Conference on Machine Learning*, pages 1597–1607. PMLR, 2020. 1, 2, 3
- [17] Xinlei Chen and Kaiming He. Exploring simple siamese representation learning. In *Proceedings of the IEEE/CVF Conference on Computer Vision and Pattern Recognition (CVPR)*, pages 15750–15758, 2021.
- [18] Xinlei Chen, Haoqi Fan, Ross B. Girshick, and Kaiming He. Improved baselines with momentum contrastive learning. *CoRR*, abs/2003.04297, 2020.
- [19] Xinlei Chen, Saining Xie, and Kaiming He. An empirical study of training self-supervised vision transformers. In *Proceedings of the IEEE/CVF International Conference on Computer Vision (ICCV)*, pages 9640–9649, 2021. 1, 2, 3, 4, 5, 6, 7, 8, 12, 17, 18, 19, 20
- [20] Rymarczyk D., Borowa ., Bracha A., Chronowski M., Ozimek W., and Zieliński B. Comparison of supervised and self-supervised deep representations trained on histological image. In *MEDINFO*, 2021. 13
- [21] Rymarczyk D., Borowa A., Tabor J., and Zielinski B. Kernel self-attention for weakly-supervised image classification using deep multiple instance learning. In *WACV*, 2021. 2, 13
- [22] Jacob Devlin, Ming-Wei Chang, Kenton Lee, and Kristina Toutanova. BERT: Pre-training of deep bidirectional transformers for language understanding, 2019. 2
- [23] Carl Doersch, Abhinav Gupta, and Alexei A. Efros. Unsupervised visual representation learning by context prediction. In *Proceedings of the IEEE International Conference on Computer Vision (ICCV)*, 2015. 2
- [24] Alexey Dosovitskiy, Lucas Beyer, Alexander Kolesnikov, Dirk Weissenborn, Xiaohua Zhai, Thomas Unterthiner, Mostafa Dehghani, Matthias Minderer, Georg Heigold, Sylvain Gelly, Jakob Uszkoreit, and Neil Houlsby. An image is worth 16x16 words: Transformers for image recognition at scale. In *International Conference on Learning Representations*, 2021. 1, 2, 3, 5, 6, 7, 8, 17, 18, 19, 20
- [25] Luyu Gao and Jamie Callan. Condenser: a pre-training architecture for dense retrieval, 2021. 3
- [26] Quentin Garrido, Mahmoud Assran, Nicolas Ballas, Adrien Bardes, Laurent Najman, and Yann LeCun. Learning and leveraging world models in visual representation learning, 2024. 2
- [27] Spyros Gidaris, Praveer Singh, and Nikos Komodakis. Unsupervised representation learning by predicting image rotations. In *International Conference on Learning Representations*, 2018. 2
- [28] Boris Ginsburg, Igor Gitman, and Yang You. Large batch training of convolutional networks with layer-wise adaptive rate scaling, 2018. 7, 12, 13
- [29] Jean-Bastien Grill, Florian Strub, Florent Altché, Corentin Tallec, Pierre Richemond, Elena Buchatskaya, Carl Doersch, Bernardo Avila Pires, Zhaohan Guo, Mohammad Gheshlaghi Azar, Bilal Piot, koray kavukcuoglu, Remi Munos, and

- Michal Valko. Bootstrap your own latent - a new approach to self-supervised learning. In *Advances in Neural Information Processing Systems*, pages 21271–21284. Curran Associates, Inc., 2020. 1, 2
- [30] Kaiming He, Xiangyu Zhang, Shaoqing Ren, and Jian Sun. Deep residual learning for image recognition. In *Proceedings of the IEEE Conference on Computer Vision and Pattern Recognition (CVPR)*, 2016. 3
- [31] Kaiming He, Georgia Gkioxari, Piotr Dollár, and Ross Girshick. Mask r-cnn, 2018. 14
- [32] Kaiming He, Haoqi Fan, Yuxin Wu, Saining Xie, and Ross Girshick. Momentum contrast for unsupervised visual representation learning. In *Proceedings of the IEEE/CVF Conference on Computer Vision and Pattern Recognition (CVPR)*, 2020. 1, 2
- [33] Kaiming He, Xinlei Chen, Saining Xie, Yanghao Li, Piotr Dollár, and Ross Girshick. Masked autoencoders are scalable vision learners. In *Proceedings of the IEEE/CVF Conference on Computer Vision and Pattern Recognition (CVPR)*, pages 16000–16009, 2022. 1, 2, 3, 4, 5, 6, 7, 8, 12, 13, 14, 17, 18, 19, 20
- [34] Yu Huang, Zixin Wen, Yuejie Chi, and Yingbin Liang. How transformers learn diverse attention correlations in masked vision pretraining. In *ICML 2024 Workshop on Theoretical Foundations of Foundation Models*, 2024. 3
- [35] Joon Seok Lee Jeong Woo Shin. Self-guided masked autoencoders. In *Master’s Thesis of Data Science*, 2023. 6, 7
- [36] Xiangwen Kong and Xiangyu Zhang. Understanding masked image modeling via learning occlusion invariant feature. In *Proceedings of the IEEE/CVF Conference on Computer Vision and Pattern Recognition (CVPR)*, pages 6241–6251, 2023. 2, 3
- [37] Hankook Lee, Kibok Lee, Kimin Lee, Honglak Lee, and Jinwoo Shin. Improving transferability of representations via augmentation-aware self-supervision. In *Advances in Neural Information Processing Systems*, pages 17710–17722. Curran Associates, Inc., 2021. 2
- [38] Tsung-Yi Lin, Michael Maire, Serge J. Belongie, Lubomir D. Bourdev, Ross B. Girshick, James Hays, Pietro Perona, Deva Ramanan, Piotr Dollár, and C. Lawrence Zitnick. Microsoft COCO: common objects in context. *CoRR*, abs/1405.0312, 2014. 2, 3
- [39] Ilse M. et al. Attention-based deep multiple instance learning. In *ICML*, 2018. 2, 7, 8, 12, 13
- [40] Mehdi Noroozi and Paolo Favaro. Unsupervised learning of visual representations by solving jigsaw puzzles. In *Computer Vision – ECCV 2016*, pages 69–84, Cham, 2016. Springer International Publishing. 2
- [41] Aaron van den Oord, Yazhe Li, and Oriol Vinyals. Representation learning with contrastive predictive coding. *arXiv preprint arXiv:1807.03748*, 2018. 1
- [42] Maxime Oquab, Timothée Darcet, Théo Moutakanni, Huy Vo, Marc Szafraniec, Vasil Khalidov, Pierre Fernandez, Daniel Haziza, Francisco Massa, Alaaeldin El-Nouby, Mahmoud Assran, Nicolas Ballas, Wojciech Galuba, Russell Howes, Po-Yao Huang, Shang-Wen Li, Ishan Misra, Michael Rabbat, Vasu Sharma, Gabriel Synnaeve, Hu Xu, Hervé Jegou, Julien Mairal, Patrick Labatut, Armand Joulin, and Piotr Bojanowski. Dinov2: Learning robust visual features without supervision. *ArXiv*, abs/2304.07193, 2023. 1, 2
- [43] Adam Pardyl, Grzegorz Rypeś, Grzegorz Kurzejamski, Bartosz Zieliński, and Tomasz Trzciński. Active visual exploration based on attention-map entropy. In *Proceedings of the Thirty-Second International Joint Conference on Artificial Intelligence, IJCAI-23*, pages 1303–1311. International Joint Conferences on Artificial Intelligence Organization, 2023. Main Track. 2
- [44] Adam Pardyl, Michał Wronka, Maciej Wołczyk, Kamil Adamczewski, Tomasz Trzciński, and Bartosz Zieliński. Adaglimpse: Active visual exploration with arbitrary glimpse position and scale. In *Computer Vision – ECCV 2024*, pages 112–129, Cham, 2025. Springer Nature Switzerland. 2
- [45] Namuk Park, Wonjae Kim, Byeongho Heo, Taekyung Kim, and Sangdoon Yun. What do self-supervised vision transformers learn? In *The Eleventh International Conference on Learning Representations*, 2023. 1, 2, 3, 6, 7, 13
- [46] Adam Paszke, Sam Gross, Francisco Massa, Adam Lerer, James Bradbury, Gregory Chanan, Trevor Killeen, Zeming Lin, Natalia Gimelshein, Luca Antiga, Alban Desmaison, Andreas Kopf, Edward Yang, Zachary DeVito, Martin Raison, Alykhan Tejani, Sasank Chilamkurthy, Benoit Steiner, Lu Fang, Junjie Bai, and Soumith Chintala. Pytorch: An imperative style, high-performance deep learning library. In *Advances in Neural Information Processing Systems 32*, pages 8024–8035. Curran Associates, Inc., 2019. 12
- [47] Zhiliang Peng, Li Dong, Hangbo Bao, Qixiang Ye, and Furu Wei. Beit v2: Masked image modeling with vector-quantized visual tokenizers, 2022. 1, 2, 3, 4, 7, 8
- [48] Marcin Przewiężlikowski, Mateusz Pyla, Bartosz Zieliński, Bartłomiej Twardowski, Jacek Tabor, and Marek Śmieja. Augmentation-aware self-supervised learning with conditioned projector. *Knowledge-Based Systems*, 305:112572, 2024. 2
- [49] Nikhila Ravi, Valentin Gabeur, Yuan-Ting Hu, Ronghang Hu, Chaitanya Ryali, Tengyu Ma, Haitham Khedr, Roman Rädle, Chloe Rolland, Laura Gustafson, Eric Mintun, Junting Pan, Kalyan Vasudev Alwala, Nicolas Carion, Chao-Yuan Wu, Ross Girshick, Piotr Dollár, and Christoph Feichtenhofer. Sam 2: Segment anything in images and videos, 2024. 2
- [50] Olga Russakovsky, Jia Deng, Hao Su, Jonathan Krause, Sanjeev Satheesh, Sean Ma, Zhiheng Huang, Andrej Karpathy, Aditya Khosla, Michael Bernstein, Alexander Berg, and Li Fei-Fei. Imagenet large scale visual recognition challenge. *International Journal of Computer Vision*, 115, 2014. 7, 8, 12
- [51] Yonglong Tian, Chen Sun, Ben Poole, Dilip Krishnan, Cordelia Schmid, and Phillip Isola. What makes for good views for contrastive learning? 33:6827–6839, 2020. 1, 2
- [52] Ashish Vaswani, Noam Shazeer, Niki Parmar, Jakob Uszkoreit, Llion Jones, Aidan N Gomez, Łukasz Kaiser, and Illia Polosukhin. Attention is all you need. In *Advances in Neural Information Processing Systems*. Curran Associates, Inc., 2017. 2, 3
- [53] Shashanka Venkataramanan, Mamshad Nayeem Rizve, Joao Carreira, Yuki M Asano, and Yannis Avrithis. Is imagenet

- worth 1 video? learning strong image encoders from 1 long unlabelled video. In *The Twelfth International Conference on Learning Representations*, 2024. [2](#)
- [54] Pascal Vincent, Hugo Larochelle, Yoshua Bengio, and Pierre-Antoine Manzagol. Extracting and composing robust features with denoising autoencoders. In *Proceedings of the 25th International Conference on Machine Learning*, page 1096–1103, New York, NY, USA, 2008. Association for Computing Machinery. [2](#), [3](#)
- [55] Pascal Vincent, Hugo Larochelle, Isabelle Lajoie, Yoshua Bengio, Pierre-Antoine Manzagol, and Léon Bottou. Stacked denoising autoencoders: Learning useful representations in a deep network with a local denoising criterion. *Journal of machine learning research*, 11(12), 2010. [1](#), [2](#), [3](#)
- [56] Chen Wei, Haoqi Fan, Saining Xie, Chao-Yuan Wu, Alan Yuille, and Christoph Feichtenhofer. Masked feature prediction for self-supervised visual pre-training, 2023. [2](#), [3](#), [4](#), [8](#)
- [57] Tete Xiao, Xiaolong Wang, Alexei A Efros, and Trevor Darrell. What should not be contrastive in contrastive learning. In *International Conference on Learning Representations*, 2021. [1](#), [2](#)
- [58] Zhenda Xie, Zheng Zhang, Yue Cao, Yutong Lin, Jianmin Bao, Zhuliang Yao, Qi Dai, and Han Hu. Simmim: A simple framework for masked image modeling. In *Proceedings of the IEEE/CVF Conference on Computer Vision and Pattern Recognition (CVPR)*, pages 9653–9663, 2022. [1](#), [2](#), [4](#), [7](#), [8](#), [12](#)
- [59] Zhenda Xie, Zigang Geng, Jingcheng Hu, Zheng Zhang, Han Hu, and Yue Cao. Revealing the dark secrets of masked image modeling. In *Proceedings of the IEEE/CVF Conference on Computer Vision and Pattern Recognition (CVPR)*, pages 14475–14485, 2023. [3](#)
- [60] xingbin liu, Jinghao Zhou, Tao Kong, Xianming Lin, and Rongrong Ji. Exploring target representations for masked autoencoders. In *The Twelfth International Conference on Learning Representations*, 2024. [3](#), [4](#)
- [61] Jason Yosinski, Jeff Clune, Yoshua Bengio, and Hod Lipson. How transferable are features in deep neural networks? In *Advances in Neural Information Processing Systems*. Curran Associates, Inc., 2014. [12](#)
- [62] Jure Zbontar, Li Jing, Ishan Misra, Yann LeCun, and Stephane Deny. Barlow twins: Self-supervised learning via redundancy reduction. In *Proceedings of the 38th International Conference on Machine Learning*, pages 12310–12320. PMLR, 2021. [1](#), [2](#)
- [63] Qi Zhang, Yifei Wang, and Yisen Wang. How mask matters: Towards theoretical understandings of masked autoencoders. In *Advances in Neural Information Processing Systems*, pages 27127–27139. Curran Associates, Inc., 2022. [1](#), [2](#), [3](#)
- [64] Richard Zhang, Phillip Isola, and Alexei A. Efros. Colorful image colorization. In *Computer Vision – ECCV 2016*, pages 649–666, Cham, 2016. Springer International Publishing. [2](#)
- [65] Jinghao Zhou, Chen Wei, Huiyu Wang, Wei Shen, Cihang Xie, Alan Yuille, and Tao Kong. Image BERT pre-training with online tokenizer. In *International Conference on Learning Representations*, 2022. [1](#), [2](#), [4](#), [5](#), [6](#), [7](#), [8](#), [12](#), [14](#), [17](#), [18](#), [19](#), [20](#)
- [66] Jiaxin Zhuang, Linshan Wu, Qiong Wang, Varut Vardhanabhuti, Lin Luo, and Hao Chen. Mim: Mask in mask self-supervised pre-training for 3d medical image analysis, 2024. [2](#), [7](#)

Appendix

A. Detailed experimental setup

In this section, we describe our experimental methodology: our choice of pretrained models, the details and hyperparameters of evaluating their representations, as well as the codebase used for the experiments.

A.1. Overview of the analyzed Vision Transformers

Our study aims to analyze the differences in representations formed by different Vision Transformer pretraining techniques. Secondly, our objective is to verify whether the aggregation of patch token representations with AbMILP can yield form better representations than those of the `[cls]` tokens.

For this purpose, we analyze various Vision Transformer architectures that were pretrained with several MIM and JEA approaches, using the parameters shared by the authors of the respective methods. This has two advantages:

- Using the existing parameters significantly reduces the computational resources required for our study.
- Our study provides insights about the *very same* sets of parameters that are described in their respective literature and used by the wider research community.

For a fair evaluation, we use the parameters of the models that were pretrained on the ImageNet-1k dataset [50]. All of the explored model parameters are compatible with the implementations of the MAE [33] or SimMIM [58] Vision Transformers. Following the MAE and DINO implementations, when using ViT-S and ViT-B, we split the image into a 14×14 grid of patches of size 16×16 . When using ViT-H, the we split the image into 16×16 patches of size 14×14 .

The only analyzed models that are not publicly available but were trained by us are the ViT-S pretrained with the MAE and the fine-tuned ViT-S/B/L variants of the MAE. To prepare these models, we used the MAE pretraining and fine-tuning codebase and hyperparameters [33]. Before fine-tuning, we initialize the model with the pretrained MAE parameters as shared by the authors and use the `[cls]` token representation as input to the classifier.

A.2. Representation evaluation details

In our evaluation of ViT representations in terms of classification accuracy, we follow the MAE linear probing protocol [33]: we augment the images only by random cropping, use the batch size of 16,384, and train the classifier head for 90 epochs (50 in the case of ViT-Large and Huge) with the LARS optimizer [28], the base learning rate of 0.1 with cosine decay and 10 epochs of warmup, optimizer momentum of 0.9, and no weight decay. When using the AbMILP learnable token aggregation, we train it alongside the classifier head.

These evaluations are performed on a single node equipped with 4 NVIDIA-GH200 GPUs. Due to the memory constraints of this setup, we obtain the effective batch size of 16,384 by aggregating gradients from two forward passes with half of that batch size.

A.3. Codebase

Our code is based on the official MAE codebase [33], written in PyTorch [46], and available at github.com/gmum/beyond_cls. We include scripts required for the analysis of the attention mechanism in ViTs, as well as linear evaluation of their representations extended with AbMILP [39].

B. Additional experimental results

B.1. Analysis of information flow in Self-supervised ViT architectures

This section contains the full experimental results of the attention mechanism in Vision Transformers, analyzed in Sec. 4. In the main manuscript, we include the analysis conducted on ViT-B, whereas in this section, we also provide the results of ViT-S and ViT-L architectures in Figures 9 to 12. For completeness, we re-include in them the pictograms describing each metric and the ViT-B results. We denote the contents of Figures 9 to 12 in Tab. 2. Due to the size of the figures, include them at the end of this supplementary material.

Analyzed models. As discussed in Appendix A.1, whenever possible, for each analyzed method, we use the ImageNet-1k pre-trained model parameters officially released by their respective authors. The only exception to this is the MAE trained with ViT-S, which we trained ourselves, and the finetuned MAE (MAE-FT), which we finetuned ourselves for ImageNet-1k classification on top of the `[cls]` token features. Due to the lack of available ViT-L parameters of MoCo-v3 [19] and DINO [14], we omit them from the analysis of this architecture. However, given that the three JEA approaches behave similarly for each property analyzed in ViT-S and ViT-B architectures, we believe that the available ViT-L iBOT [65] variant sufficiently represents JEA. Similarly, we do not conduct this comparison with the ViT-H architecture, due to the lack of publicly available parameters of ViT-H trained with JEA to compare with.

Discussion. We are interested in the behavior of the ViT attention mechanism emergent in the MAE and JEA approaches, especially in the deep ViT blocks which form higher-level image representations [61]. Across the three ViT architectures analyzed, we observe several consistent trends, more generally discussed in Section 4.3 and summarized below:

Metric	ViT-B results (manuscript)	ViT-S/B/L results (Appendix)
[cls]-[cls] attention	Fig. 3	Fig. 9
[cls]-patch entropy	Fig. 4	Fig. 10
patch-patch attention	Fig. 5	Fig. 11
patch-patch entropy	Fig. 6	Fig. 12

Table 2. A reference of Figures depicting the analysis of the attention mechanism and their extended counterparts in the Appendix.

- The [cls] token of pretrained and fine-tuned MAE assigns a large portion of attention (around 40-50%) to its own representation.
- The entropy of attention between the [cls] and patch tokens is much higher in MAE than in the rest of the models, indicating that it aggregates the information from a larger number of patch tokens. Fine-tuning of the MAE decreases this value to the levels observed in JEA models, increasing the selectiveness of attention.
- The attention of MAE patch tokens to themselves (relative to all patch tokens) is higher than in other models, indicating they are more likely to preserve their own, diverse information [45]. Fine-tuning of the MAE results in lowering this metric to the level observed in the JEA and supervised models. MAE patches also attend to other patches with lower entropy than in JEAs and this does not change after fine-tuning.

B.2. Designing the token aggregation mechanism

In this section, we discuss different design choices for the token aggregation function, which uses either various variants of AbMILP [39], or other, non-trainable substitutes. All experiments reported in this section are conducted with the ViT-B model pre-trained with the MAE [33].

Ablation study of AbMILP variants. We explore several designs of the model used by AbMILP to predict the scores for patch aggregation and report their performance in Tab. 3.

AbMILP variant	Accuracy
2-layer MLP + Tanh	68.70
2-layer MLP + ReLU	71.65
1 linear layer	71.58
SA-AbMILP [21]+SGD	74.83

Table 3. Comparison of ImageNet-1k classification accuracy of the MAE representation aggregated by different variants of AbMILP [39], including SA-AbMILP [20].

The original AbMILP architecture [39] uses a 2-layer MLP with the Tanh activation function. MAE patch tokens

aggregated by this model achieve an accuracy of 68.70. Although this is higher than the [cls] token representation, we found that the training process is unstable and replaced the Tanh activation with ReLU. This led to more stable training and an improvement in accuracy by almost 3 pp. Surprisingly, reducing the MLP to a single linear layer achieves almost the same results. Due to the simplicity and performance of this design, we adopt it in our main experiments. As seen in Sec. 5.1, the effectiveness of this approach generalizes to aggregating representations of MIM models other than the MAE.

We note that AbMILP is just one of several Multiple-Instance Learning methods that can be adopted to aggregate patch token representations. As an alternative, we explore the Self-Attention AbMILP [20] where, prior to computing the aggregation scores and the aggregated representation, tokens are processed by an additional trainable self-attention head. This approach achieves accuracy much closer to that of the JEA-trained approaches – 74.83%. This indicates an even larger richness of information stored in the representation space of Masked models, which requires more complex task-specific heads in order to be fully exploited. However, we found the training of this model to be unstable with the LARS optimizer [28], and were only able to train it using SGD. Moreover, a classification head that internally uses trainable self-attention to pre-process the classifier input is incomparable to a simple linear probe. For these reasons, we do not include this approach in our main experiments.

Non-trainable token aggregation. Apart from the AbMILP-based aggregation, we explore several alternative token aggregation functions that are not trained along with the classifier model. We discuss these approaches and their properties below and report their representations’ average accuracies and entropies of the aggregation vectors in Tab. 4. To measure if different token aggregation approaches select the same patch tokens, in Fig. 7, we report the average Kullback-Leibler Divergence between token selection vectors produced by each method. Finally, we visualize the example token selection vectors in Fig. 8.

- **Average MAE [cls] token attention** – the average attention between the [cls] and patch tokens, produced by the MSA of the final MAE ViT block. As evidenced by the high entropy, this approach aggregates many patches, achieving quality similar to that of the regular [cls] representation.
- **Lowest-entropy MAE [cls] token attention** – the attention map between the [cls] and patch tokens produced by the MSA of the final MAE ViT block, which has the lowest entropy. This approach achieves low aggregation entropy, but due to the diversity of image fragments attended by different self-attention heads [45], the attended fragment of an image is not guaranteed to contain the object of interest.

- **MAE central patch token attention** – the average attention between the token of the central patch in the image and other patches. This approach can distinguish the tokens of the object of interest as long as it is depicted on the central image patch, which is not always the case. As evidenced by the high KLD between the Lowest-entropy MAE [cls] token attention and MAE central patch token attention, these two approaches tend to have a low agreement in terms of which tokens to select, suggesting their high volatility.
- **Average DINO [cls] token attention** – the average attention between the [cls] and patch tokens, produced by the MSA of the final DINO ViT block. As observed by [14], DINO attention maps are exceptionally good at capturing the main objects of interest in the images. MAE patch tokens selected with this approach form representations superior to the [cls] token, but an obvious drawback of this approach is the reliance on an externally pre-trained model. As seen in Fig. 7, this selects tokens most similar to the AbMILP-based token aggregation.

Token aggregation approach	Accuracy	Entropy
Average MAE [cls] token attention	67.8	5.14
Lowest-entropy MAE [cls] token attention	66.3	4.77
MAE central patch token attention	65.2	4.70
Average DINO [cls] token attention	70.9	4.89
AbMILP	71.6	4.80

Table 4. Evaluation of different token aggregation approaches in terms of classification accuracy of their representations, and entropy of the aggregation vectors they produce.

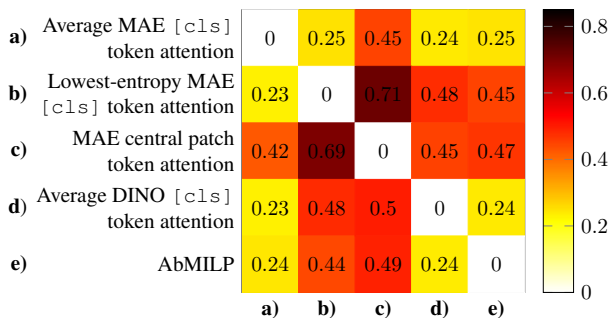


Figure 7. Mean KLD between aggregation vectors produced by different token aggregation techniques.

Most of the above approaches select the MAE patch tokens with an entropy close to that observed in the JEA [cls] token. However, except for the attention maps generated by DINO and AbMILP, we did not find an approach that would reliably select patch tokens to form a representation of better quality than the [cls] token. Finding such tokens in an unsupervised manner is an interesting direction for future work.

B.3. Impact of patch token quality and overfitting for classification in dense prediction tasks

In this section, we evaluate the influence of the pretraining task on the *out-of-the-box* quality of ViT representations in dense prediction tasks. We also evaluate the impact of tuning the MAE encoder for more selective representation aggregation, in the form of MAE previously fine-tuned for classification on top of the [cls] representation.

To this end, we evaluate the DINO [14], MAE [33], and MAE (fine-tuned) ViT-B encoders on the tasks of object detection and instance segmentation on the COCO dataset [38]. We follow the experimental setup, hyperparameters, and the codebase of iBOT [65], who use Mask R-CNN [31] as the object detector. However, since we are interested in the out-of-the-box performance of ViT encoders, we train only the object detection module and leave the encoder parameters frozen. Moreover, since we are interested in the performance of final ViT representations, the detector module takes as the input feature maps formed the final ViT block patch tokens. We report the Average Precision results in Table 5. It is evident that the out-of-the-box representations formed

Encoder	AP _l ^b	AP _m ^b	AP _s ^b	AP _l ^m	AP _m ^m	AP _s ^m
DINO	0.472	0.353	0.205	0.467	0.312	0.149
MAE	0.413	0.32	0.186	0.417	0.292	0.140
MAE (FT)	0.433	0.308	0.172	0.425	0.272	0.122

Table 5. Average precision of box (^b) and mask (^m) predictions of large, medium, and small objects from the COCO dataset. To assess the quality of out-of-the-box network representations, we train object detectors on the feature maps produced by final ViT patch token representations without training the encoders themselves.

by DINO are better suited for dense prediction than those of the MAE. We attribute this to the low-level prediction target of the MAE that results in less descriptive patch representations [8]. Furthermore, fine-tuning of the MAE for classification on top of the [cls] features, *decreases* its ability to distinguish medium and small objects. This shows that fine-tuning, which improves the representation aggregation ability of the MAE, can also negatively affect its usefulness for other visual tasks.

Our work focuses primarily on the global representation aspect of MIM models and less so on dense prediction tasks. However, the above results show that the improved performance on one can adversely impact the other. The development of representation aggregation solutions that can also maintain the quality of local patch representations is a vital question for future research.

C. Future research directions

Our results indicate that lack of global representation aggregation is inherent to Vision Transformers trained with

Masked Image Modeling. In this section, we summarize several potential research directions for better understanding this issue.

Unsupervised discovery of relevant tokens. In Section 5, we show that there exists a function for recognizing the patch tokens of MIM models that are relevant to form global image representations. Moreover, it can be expressed with a shallow model. However, in each MIM model, we learn that function together with the classifier dedicated to downstream tasks. Understanding what makes a patch token relevant for global representation and finding such tokens in an unsupervised manner is a natural further direction.

Global and dense prediction trade-off. Appendix B.3 shows that overfitting a model for global representation can adversely affect its dense prediction capabilities. Although our work strongly motivates the integration of the representation aggregation and Masked modeling objectives, works on this topic should avoid creating mechanisms which decrease the models' dense prediction capabilities in favor of better global representations.

Aggregation of internal ViT representations. In this work, we have made the implicit assumption that the aggregation function should only act on patch representations of the final ViT block. Although the explored AbMILP approach improves the MIM representations, we note that it does not interfere in any way with their internal information flow. However, as shown in Fig. 4, the [cls] token of JEAs aggregates patch information increasingly selectively throughout the several final model blocks. We hypothesize that similarly aggregating MIM representations within internal ViT blocks, either via additional training objectives or post hoc modifications, could yield further improvements in their quality.

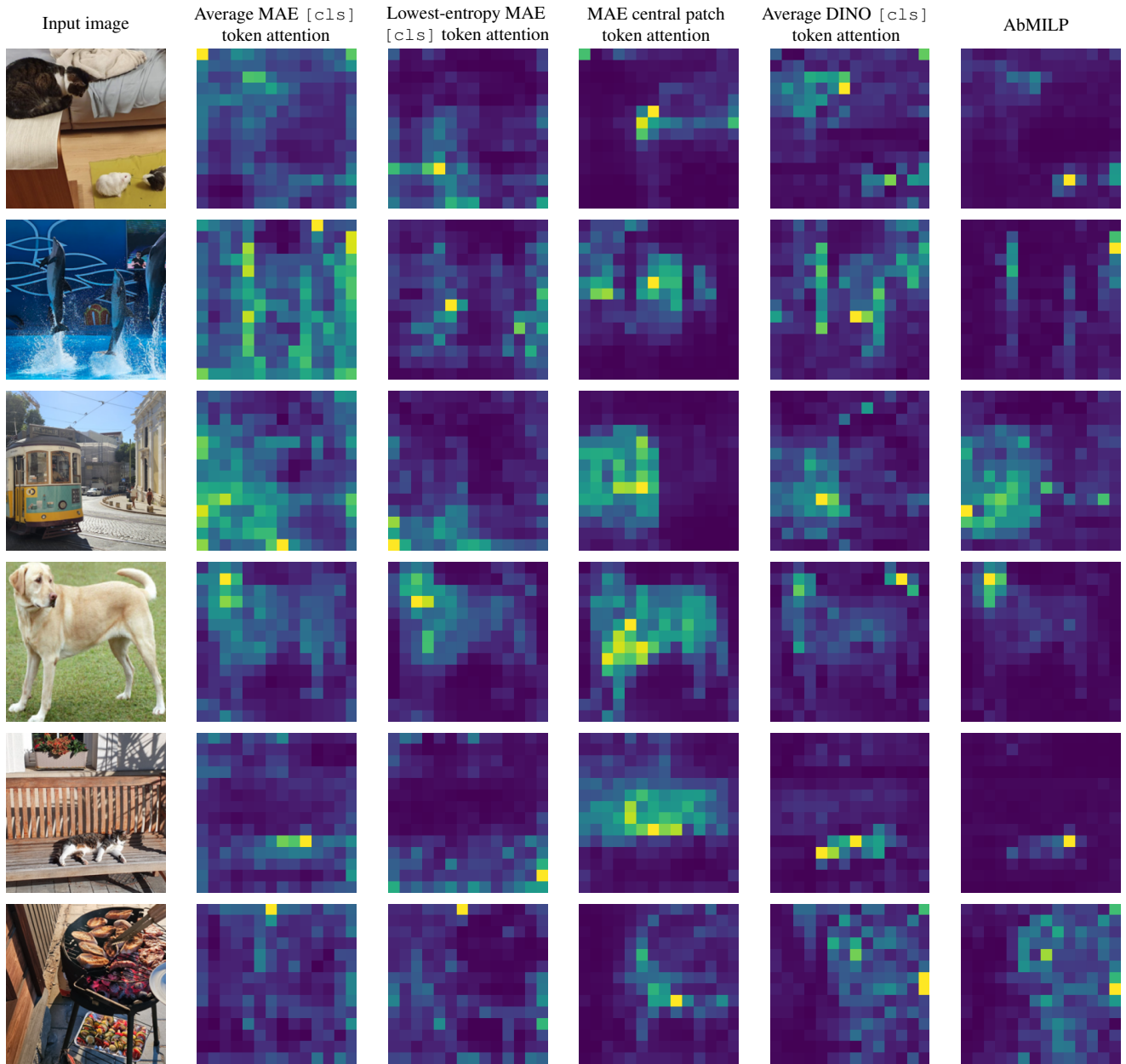


Figure 8. Example token aggregation scores produced by different approaches denoted in columns. The average [cls] attention of the MAE aggregates the patches too uniformly. The [cls] attention with lowest entropy and the attention of the central patch have low entropy, but are not guaranteed to capture the object of interest in the image. Finally, the DINO [cls] attention maps and aggregation vectors produced by AbMILP reliably identify the most crucial patches for forming high-level global image representations.

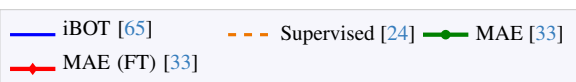
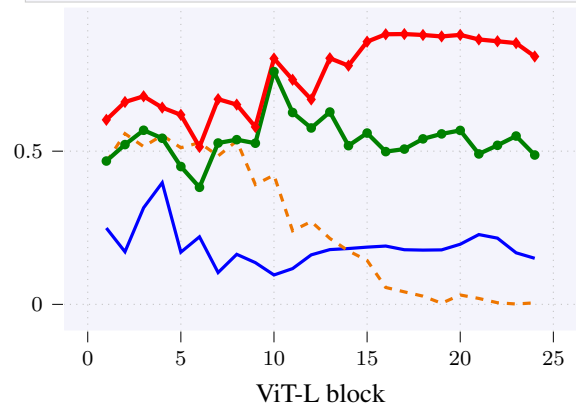
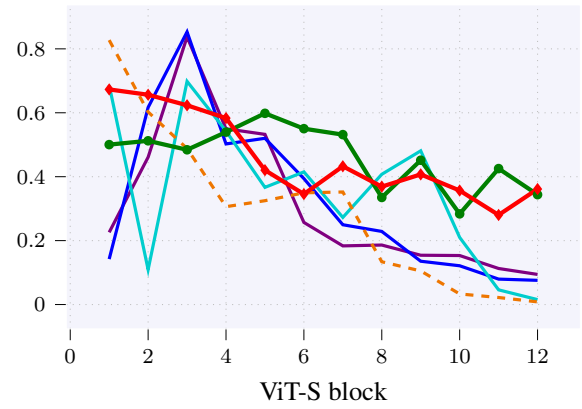
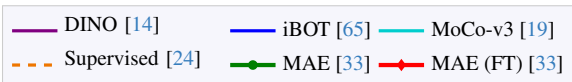
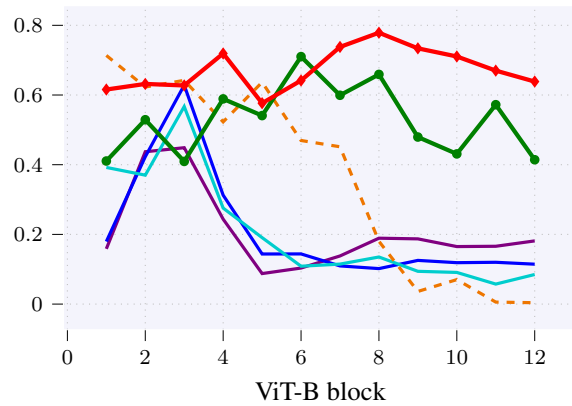
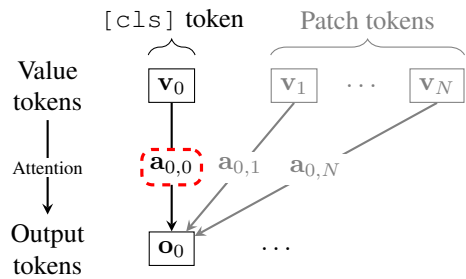


Figure 9. Extended version of Figure 3. Attention of the [cls] token to itself is much higher in both pretrained and finetuned MAE, than in the JEA ViTs. As opposed to JEA, where the [cls] tokens gather a large amount of information from the patch tokens, the MAE [cls] token primarily recycles its own representation.

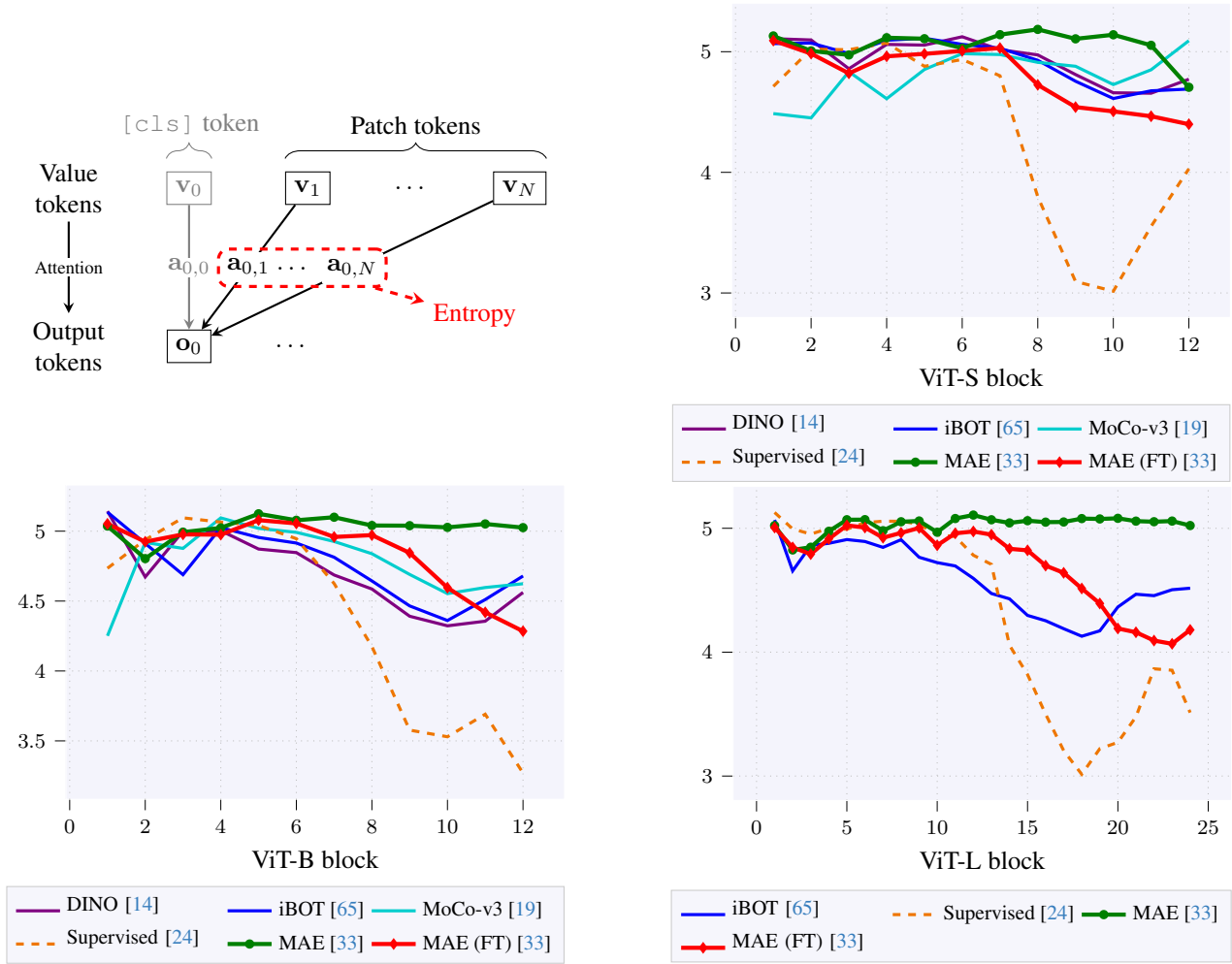


Figure 10. Extended version of Figure 4. Entropy of attention between the `[cls]` and patch tokens. In MAE, its value reaches almost the maximal possible level, In other models, it decreases in the deeper model blocks, indicating that the `[cls]` token attends to different patches in a more selective manner. Fine-tuning of MAE decreases this entropy, indicating that selective attention to patch tokens is crucial for good perception.

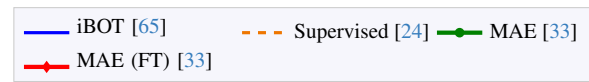
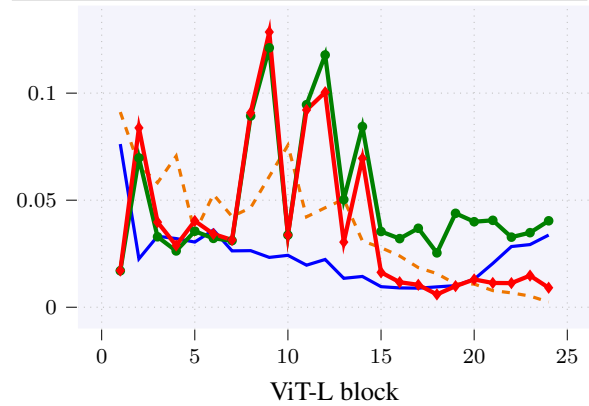
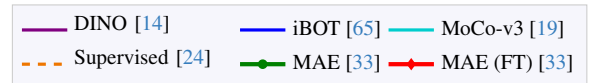
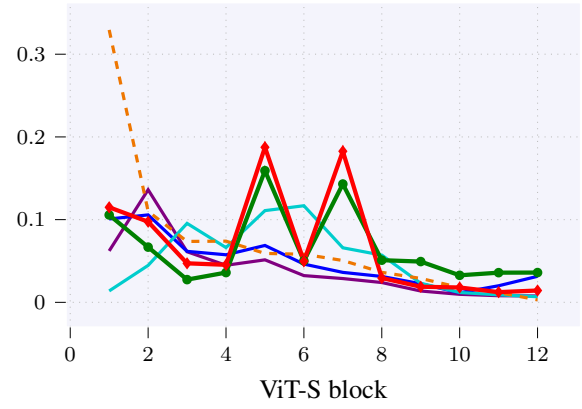
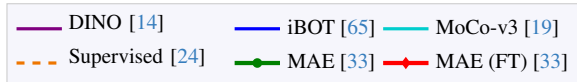
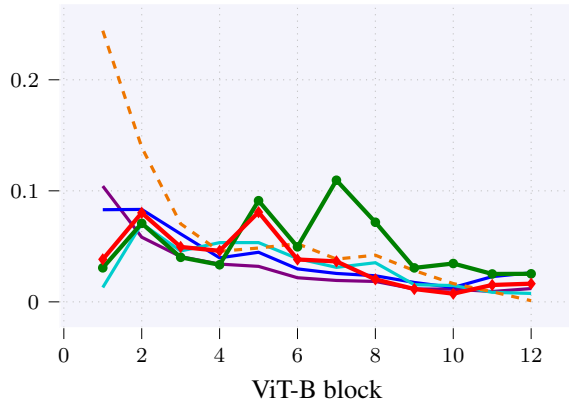
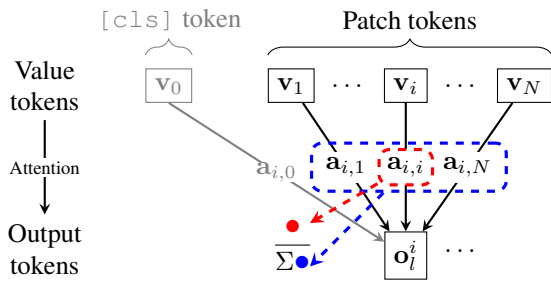


Figure 11. Extended version of Figure 5. Attention of the patch tokens to themselves, relative to the total attention assigned to all patch tokens. In the latter MAE blocks, patch tokens seem to assign the largest amount of relative attention to themselves, compared to the tokens of JEA.

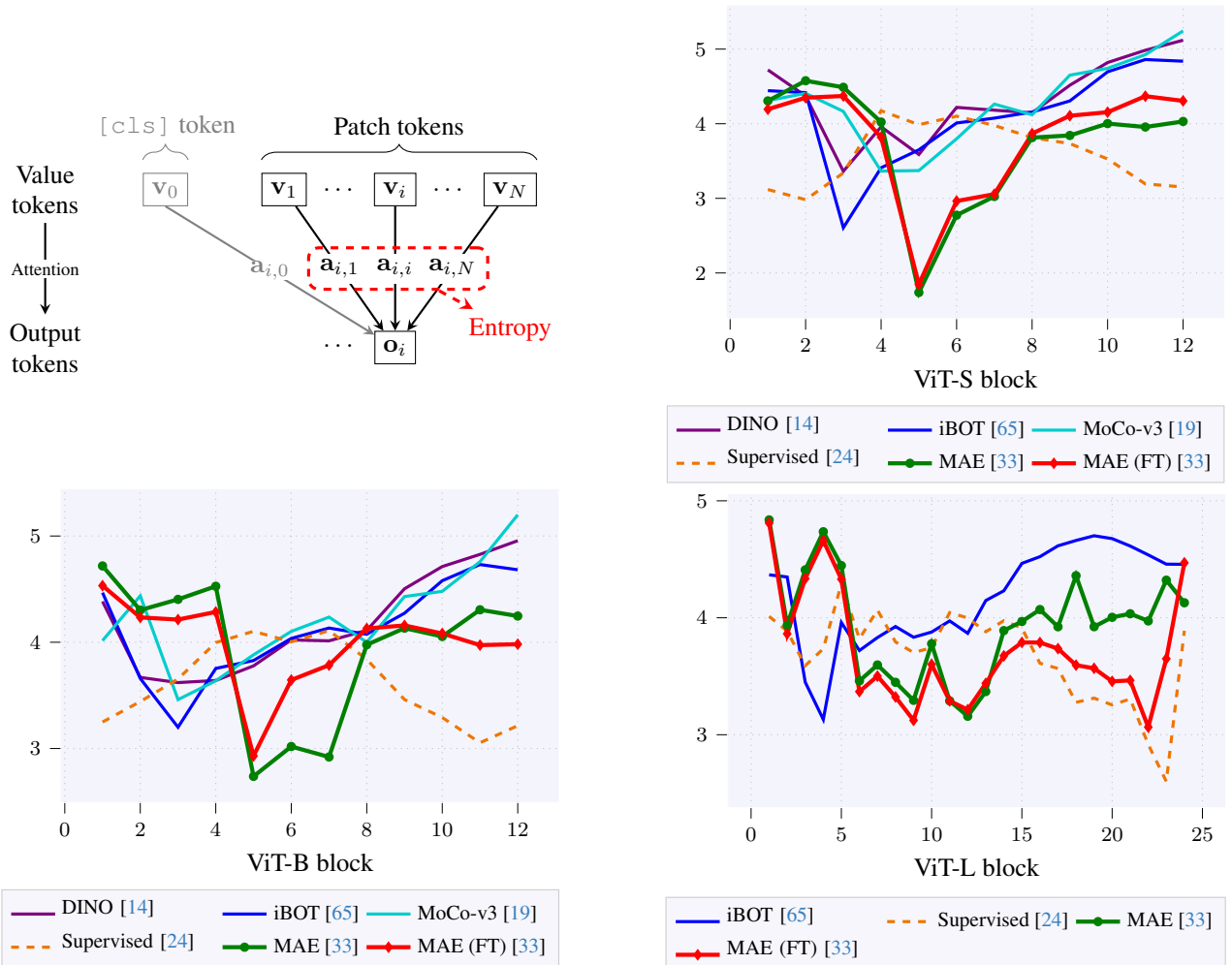


Figure 12. Extended version of Figure 6. Entropy of attention of patch tokens to patch tokens. In MAE, the patch tokens attend to other patches with lower entropy than in JEA, suggesting that they form a representation of their local image fragments.